Supporting Information

Ultrathin Metal-Organic Framework Nanosheet Arrays and Derived Self-Supporting Electrodes for Overall Water Splitting

Yanru Wang, Ani Wang,* Zhenzhen Xue, Xiaoyu Li and Guoming Wang*

KEYWORDS: Metal-Organic Framework, 2D MOF nanosheet, Self-Supporting Electrode, Hydrogen Evolution Reaction, Oxygen Evolution Reaction, Overall Water Splitting

College of Chemistry and Chemical Engineering, Qingdao University, Shandong 266071, P. R. China

Corresponding Author: *Guoming Wang

E-mail address: gmwang_pub@163.com

Experimental section

Materials

Cobalt nitrate hexahydrate ($Co(NO_3)_2 \cdot 6H_2O$), Nafion solution (5 wt%), commercial Pt/C, 2,5-bis(1-imidazol)pyridine (bimpy), *p*-phthalic acid (*p*-H_2bdc), ruthenium dioxide (RuO_2), and potassium hydroxide (KOH) were purchased from Aladdin Ltd. (China). Polyvinyl pyrrolidone (PVP, Mw = 1300000) was purchased from Shanghai Titan Scientific Co., Ltd. Methanol was purchased from Tianjin Fengchuan Chemical Reagent Co., Ltd. Ni foam was purchased from CeTech Co., Ltd. All these reagents were analytical grade and used without any further purification.

Synthesis of Ni@CoO Nanowall array

The CoO nanowall array was synthesized on Ni foam by a hydrothermal reaction. In detail, 582 mg of cobalt nitrate hexahydrate, 600 mg of urea, and 296 mg of ammonium fluoride were dissolved in 36 mL of deionized water. The homogeneous solution obtained was transferred into a Teflon-lined stainless steel autoclave with a piece of clean nickel foam (4×3×3.5 cm) immersed into the reaction solution. The autoclave was sealed and maintained at 120℃ for 10 hr and then cooled down to room temperature. The array sample was collected and rinsed with distilled water several times and then directly annealed at 350℃ in N_2 gas for 1 hr at a heating rate of 2℃/min.

Synthesis of Ni@CoO@Co-MOF

Typically, a piece of Ni@CoO nanowall array (1 × 1 cm) was added into 10 mL of deionized water containing *p*-benzene dicarboxylic acid (20 mg). After stirring for 30 min at room temperature, polyvinylpyrrolidone (4 mg) and 2,5-bis(1H-imidazol-1-yl)pyridine (20mg) were added into the above solution and stirred for 1 h at 90℃. Finally, the array sample was collected and rinsed with distilled water several times and then dried in an oven at 85℃ for 12 hr to give Ni@CoO@Co-MOF.

Synthesis of Ni@CoO@Co-MOFC

The synthesized Ni@CoO@Co-MOF were transferred into a ceramic boat and placed into a temperature-programmed furnace under an N_2 atmosphere. After several vacuuming-filling N_2 cycles at room temperature, the carbonization of the composites was performed at 400 °C for 2 h with a heating ramp rate of 10 °C min^{-1} from the room temperature. After cooling to room temperature, the resulting samples were labelled as Ni@CoO@Co-MOFC.

Characterization

Details of the X-ray crystallography.

The structural data of the compounds were collected on a XtaLAB Mini (ROW) diffractometer at room temperature. Then solved and refined by direct methods and full-matrix least-squares on F^2 using the SHELX-2014 program, respectively. All non-hydrogen atoms were refined anisotropic thermal parameters. CCDC 2072472 contains the supplementary crystallographic data for Co-MOF in this paper. The detailed crystallographic data together with structure determination summaries for the compounds are listed in Table S1.

Details of the physical measurements.

X-ray diffraction (XRD, Bruker D8 Advance, scan range of 5–50°) analyses were utilized to determine the crystal structure. Scanning electron microscope (SEM, Hitachi, S2400) and transmission electron microscopy (TEM, FEI Talos F200S) equipped with energy dispersive spectroscopy (EDS) detector were used to investigate the microstructures of all the prepared samples. Specifically, the sample was stripped from Ni foam for TEM observation to gain the detailed microstructure information. X-ray photoelectron spectroscopy (XPS) was tested on the Escalab 250Xi electron spectrometer.

Electrochemical measurements

All electrochemical measurements were tested on a CHI 760E electrochemical workstation coupled with a typical three-electrode system in 1.0 M KOH solution at room temperature. The as-synthesized electrocatalysts with the geometric area of 1 × 1 cm^2 were directly used as working electrodes, while a Hg/HgO electrode were employed as the reference and counter electrodes, respectively. The OER and HER performances were recorded by linear sweep voltammetry (LSV) curves in the N_2-saturated electrolyte with the scan rate of 5 mV s^{-1}. For control experiments, homodisperse commercial RuO_2 and Pt/C (3 mg of powder in 300 μL of ethanol and 10 μL of 5 wt% Nafion) were loaded onto the clean Ni foam as working electrodes, which have the equivalent loading amount with the afore-mentioned samples. The Hg/HgO reference electrode was calibrated against the reversible hydrogen electrode (RHE) in 1 M KOH. The RHE was designated as the working electrode, and a Pt wire was used as the counter electrode. The experimentally measured offset value for the Hg/HgO against the RHE was found to be 0.923 V. All polarization curves involved in this study were corrected for 85% iR compensation. Tafel plots are acquired in linear regions through fitting *via* Tafel equation ($\eta = a + b \log j$), where η is the overpotential, b represents the Tafel slope, and j is the current density. Electrochemical impedance spectroscopy (EIS) researches were recorded ranging from 0.01 to 10^5 Hz at overpotentials of 10 mV with an amplitude perturbation of 5 mV. Double-layer capacitance (C_{dl}) data were conducted by cyclic voltammetry (CV) curves at increasing sweep rate from 10 to 200 mV s^{-1}. The electrochemical stability tests were examined by multistep chronopotentiometry curves at the current densities of 10, 20, and 50 mA cm^{-2} for 25 h.

The significance of the reference calibration electrode is to make the measured data

more accurate and repeatable, and to minimize human errors. In this work, H_2 purging was used to calibrate the reference electrode. The principle of H_2 correction is that the hydrogen evolution reaction (HER) reaction occurs when the voltage is less than 0V vs RHE, the hydrogen oxidation reaction (HOR) reaction occurs when the voltage is greater than 0 V, and the current is 0 A when the voltage is 0 V. Use Hg/HgO (SHE 0.098V) electrode and 1 M KOH electrolyte to describe the calibration process in detail.

The steps are as follows:

a) Find a useful Hg/HgO reference electrode.

b) Estimate the potential interval. According to the estimation of E(RHE) = E(SHE) + 0.059 pH, in 1 M KOH, what is the approximate value of E(RHE) (0.924 V for Hg/HgO);

c) Equipped with electrolyte. (1 M KOH)

d) Purging with pure H_2 for 30 minutes. (Be sure to pay attention to safety! Use a fume hood and a gas sensor. The time is related to the flow rate. If it is too small, consider air backflow. If the electrolyte is too large, it will evaporate. It is recommended to seal with plastic wrap.)

e) Connect the circuit. Both the working electrode and the counter electrode are made of platinum, and the reference electrode is Hg/HgO;

f) 0 A point test. The electrochemical workstation makes a CV curve around the estimated E(RHE) value, Pre-scan to find the approximate position of 0 A, -0.875~-0.975V, the scanning speed can be 5 $mV \cdot s^{-1}$, and it is found that the potential of 0 A is about -0.924 V; Reduce the CV range: -0.915~-0.935V, sweep speed 1$mV \cdot s^{-1}$, take the average of the positive and negative sweep intersection points, and the general difference is 1mV. Pay attention to the test at least 3 times. If the coincidence is not good, it means that the H_2 purge is insufficient. Increase

the flow and continue to step d.

Table S1. Selected bond distances (Å) and angles (°) for Co-MOF

Co-MOF			
Co(1)-O(3)	2.034 (2)	O(1)-C(13)-O(2)	121.0(2)
Co(1)-N(1)	2.095 (2)	O(1)-C(13)-C(14)	119.7(3)
Co(1)-N(3)	2.120(2)	O(2)-C(13)-C(14)	119.4(3)
Co(1)-O(5)	2.1526(19)	O(4)-C(17)-O(3)	125.7(3)
Co(1)-O(1)	2.1865(18)	O(4)-C(17)-C(18)	117.5(3)
Co(1)-O(2)	2.209(2)	O(3)-C(17)-C(18)	116.7(2)
C(13)-O(1)	1.253(4)	O(3)-Co(1)-N(1)	93.21(9)
C(13)-O(2)	1.270(3)	O(3)-Co(1)-N(3)	91.04(9)
C(1)-N(1)	1.295(4)	N(1)-Co(1)-N(3)	91.05(9)
C(1)-N(2)	1.351(3)	O(3)-Co(1)-O(5)	91.20(8)
C(2)-N(1)	1.380 (3)	N(1)-Co(1)-O(5)	93.53(8)
C(3)-N(2)	1.378(4)	N(3)-Co(1)-O(5)	174.78(8)
C(4)-N(2)	1.423(4)	O(3)-Co(1)-O(1)	109.74(8)
C(17)-O(4)	1.240(4)	N(1)-Co(1)-O(1)	157.05(9)
C(17)-O(3)	1.259(4)	N(3)-Co(1)-O(1)	88.63(8)
C(7)-N(3)	1.304(4)	O(5)-Co(1)-O(1)	86.17(7)
C(7)-N(4)	1.358(4)	O(3)-Co(1)-O(2)	168.87(8)
C(8)-N(4)	1.374(4)	N(1)-Co(1)-O(2)	97.16(9)
C(9)-N(3)	1.380(4)	N(3)-Co(1)-O(2)	92.80(9)
C(10)-N(4)	1.418(4)	O(5)-Co(1)-O(2)	84.14(7)
O(1)-C(13)-O(2)	121.0(3)	O(1)-Co(1)-O(2)	59.95(7)
O(1)-C(13)-O(2)	121.0(2)	C(1)-N(1)-C(2)	106.0(2)
O(1)-C(13)-C(14)	119.7(3)	C(1)-N(1)-Co(1)	125.83(19)
O(2)-C(13)-C(14)	119.4(3)	C(2)-N(1)-Co(1)	128.1(2)
C(3)-C(2)-N(1)	109.5(3)	C(1)-N(2)-C(3)	106.4(3)
C(2)-C(3)-N(2)	106.3(2)	C(1)-N(2)-C(4)	126.1(3)
C(6)-C(4)-N(2)	117.6(3)	C(3)-N(2)-C(4)	127.3(2)
C(5)-C(4)-N(2)	120.6(3)	C(7)-N(3)-C(9)	105.6(2)
N(3)-C(7)-N(4)	111.6(3)	C(7)-N(3)-Co(1)	125.2(2)
C(9)-C(8)-N(4)	106.2(3)	C(9)-N(3)-Co(1)	129.1(2)
C(8)-C(9)-N(3)	109.9(3)	C(7)-N(4)-C(8)	106.6(2)
C(12)-C(10)-N(4)	118.3(3)	C(7)-N(4)-C(10)	125.8(3)

C(11)-C(10)-N(4)	120.3(3)	C(8)-N(4)-C(10)	127.5(3)

Table S2. Crystallographic and structural data for Co-MOF.

	Co-MOF
CCDC No.	2072472
Formula	C19 H15 Co N5 O5
Mr	452.29
Crystal system	Triclinic
Space group	*' P-1'*
a [Å]	8.4357(9)
b [Å]	9.7799(8)
c [Å]	12.6121(13)
α [˚]	68.832(9)
β [˚]	89.761(9)
γ [˚]	77.900(8)
Volume [Å^3]	945.81(17)
Z	2
D_c [g·cm^{-3}]	1.588
μ [mm^{-1}]	0.951
F (000)	462
Θ range [˚]	2.912–25.199
h range	–10<=*h*<=10
k range	–11<=*k*<=11
l range	–15<=*l*<=15
data/restraints/params	3396 / 0 / 279
GOF	0.973
R_1, wR_2[I>2σ(I)][a]	0.0410, 0.0884
R_1, wR_2[all data][a]	0.0687, 0.0947
$\Delta\rho_{max}$, $\Delta\rho_{min}$ [e·Å^{-3}]	0.593, -0.320

[a] $R_1 = \sum||F_o| - |F_c||/\sum|F_o|$; $wR_2 = [\sum[w\,(F_o^2 - F_c^2)^2]/\sum[\,w\,(F_o^2)^2]]^{1/2}$.

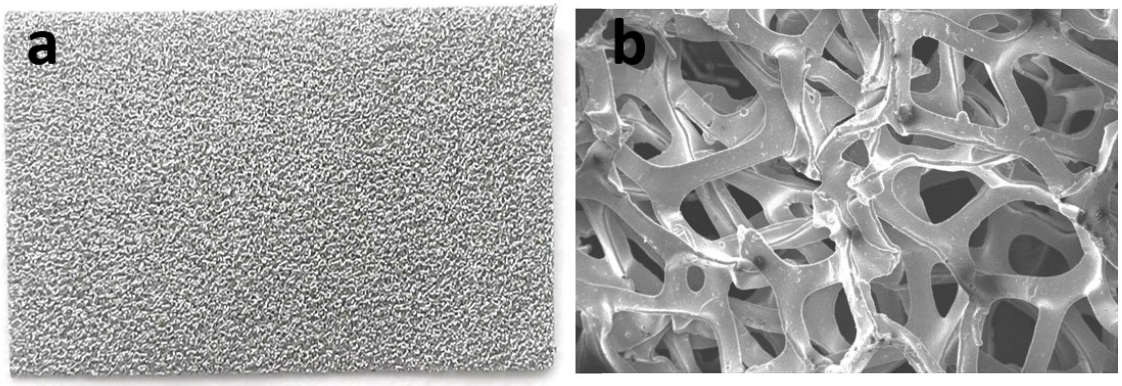

Figure S1. (a) The photo of the Ni foam. (b) SEM images of the Ni.

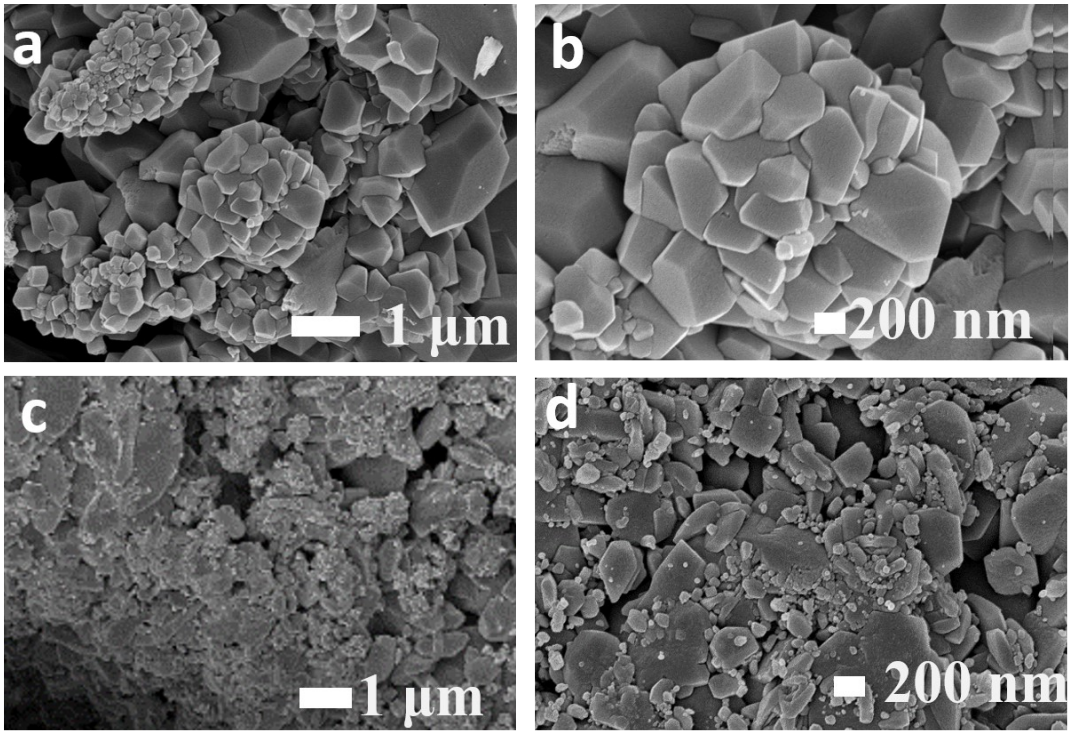

Figure S2. SEM images of crystalline Co-MOF obtained by (a and b) hydrothermal method without Ni foam and (c and d) with and Ni foam.

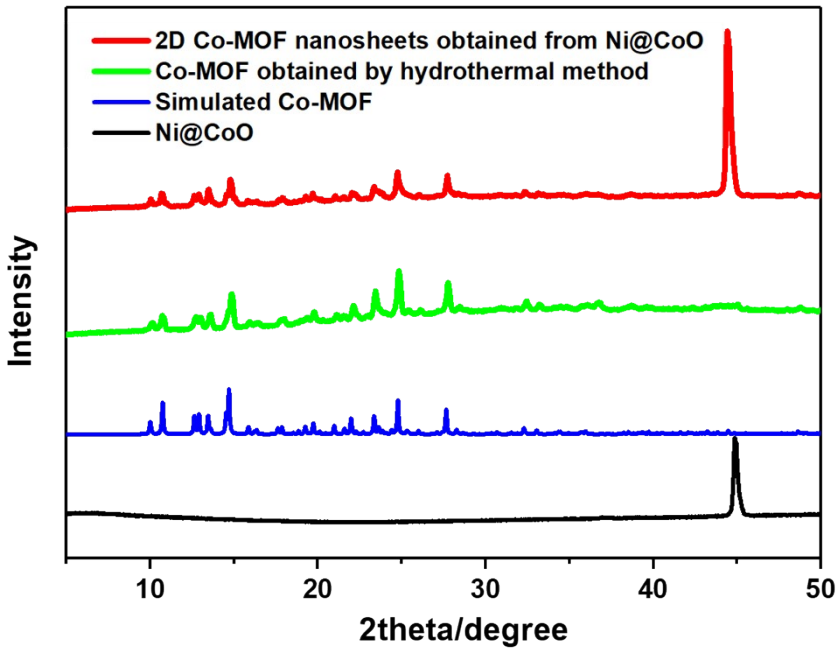

Figure S3. Powder X-ray diffraction patterns of the 2D Co-MOF nanosheets, the bulk Co-MOF obtained by hydrothermal method, the simulated Co-MOF and Ni@Co.

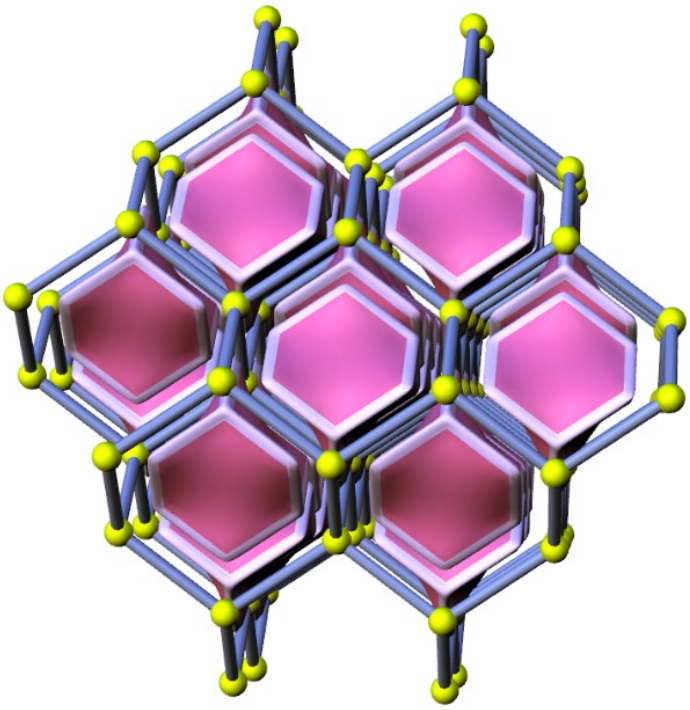

Figure S4. 4-connected ***dia*** topolgy network with the point symbol of $\{6^6\}$ for Co-MOF.

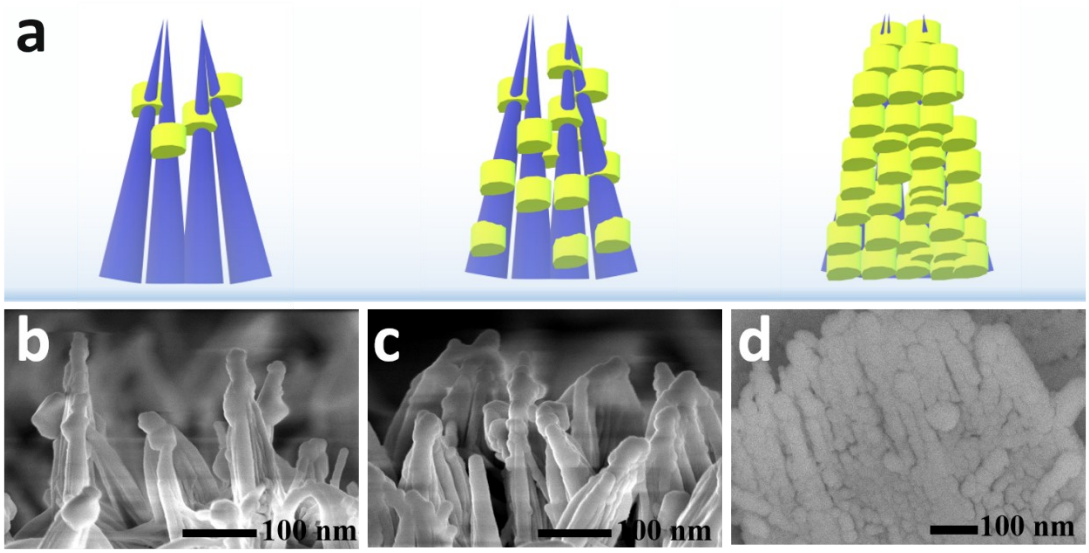

Figure S5. (a) Schematic illustration process of growth for 2D MOF nanosheets from Ni@CoO. (b-d) SEM images taken every 10 minutes to track the process of growth (10 min, 20 min and 30 min).

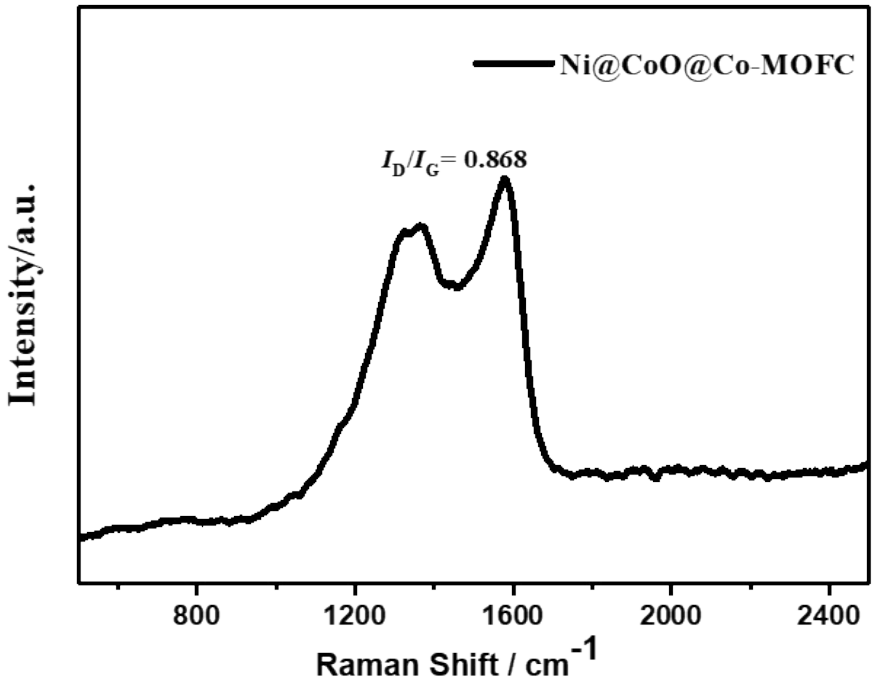

Figure S6. Raman spectroscopy of the Ni@CoO@Co-MOFC.

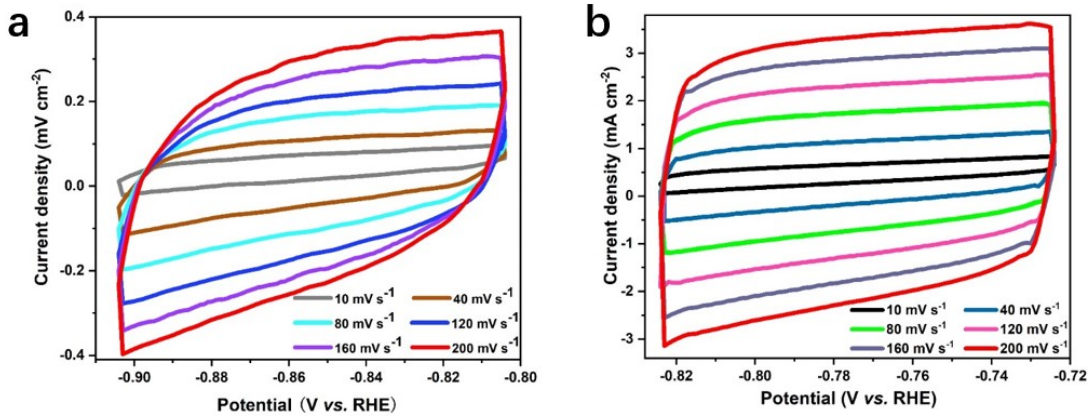

Figure S7. CV curves of (a) Ni@CoO@Co-MOF and (b) Ni@CoO measured in 1 M KOH at various scan rates (10–200 mV s^{-1}).

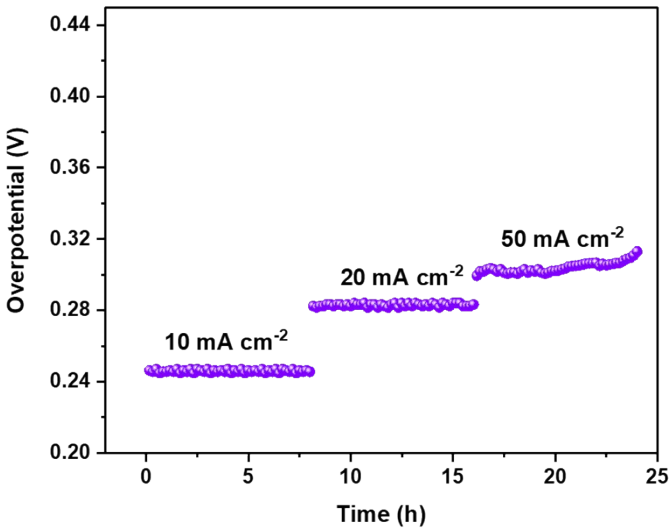

Figure S8. Long-term durability measurement of Ni@CoO@Co-MOFC.

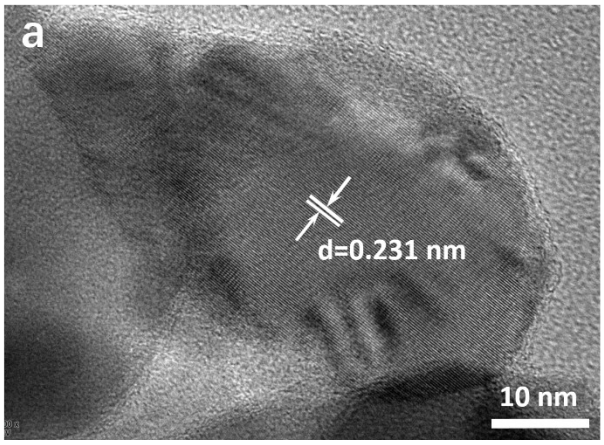

Figure S9. (a) HRTEM images of for Ni@CoO@Co-MOFC after continuous electrolyzing for OER over 24 h.

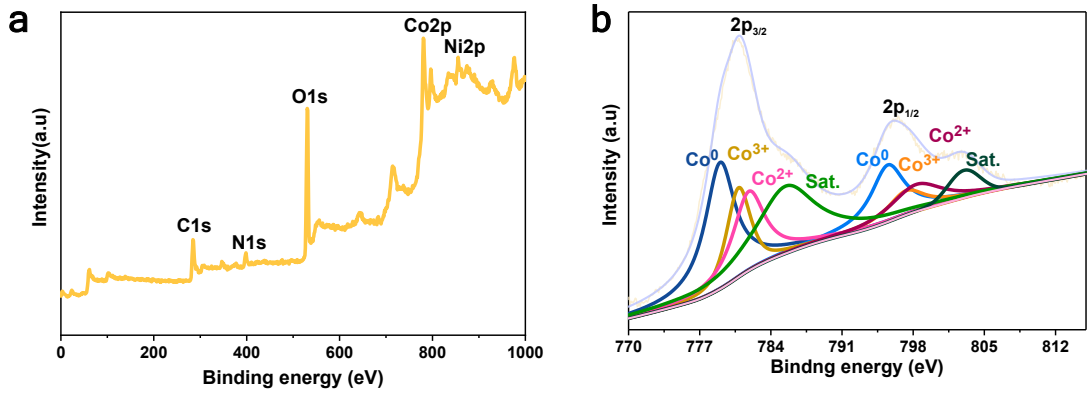

Figure S10. (a) XPS patterns of Ni@CoO@Co-MOFC after stability test. (b) Co 2p high-resolution XPS spectra of Ni@CoO@Co-MOFC after the stability.

Table S3. Summary of Co and CoO-based materials for HER in alkaline media. (η_{10}-overpotential at 10 mA cm^{-2})

Catalysts	Electrolyte	η_{10}(mV)	Tafel slope (mV dec^{-1})	Refs.
EG/$Co_{0.85}$Se/NiFe-LDH	1 M KOH	260	160	[1]
Co@CNF	1 M KOH	196	96	[2]
N-Co@G	0.1 M NaOH	337	-	[3]
Co-NC/CNT	1 M KOH	203	125	[4]
CoO@Co/N-rGO	0.1 M KOH	237	-	[5]
Co-NRCNTs	1 M KOH	370	-	[6]
Co@NG	1 M KOH	220	112	[7]
Co/CoP-5	1 M KOH	253	73.8	[8]
CoO_x@CN	1 M KOH	232	-	[9]
CF–NG–Co	1 M KOH	212	75	[10]
Co_9S_8@C	1 M KOH	250	-	[11]
Fe-doped CoP	1.0 M KOH	230	75	[12]
H-CoP@NC	1.0 M KOH	200	71	[13]
CoP/CC	1.0 M KOH	209	129	[14]
CP/CTs/Co-S	1.0 M KOH	190	131	[15]
CoNiP@NF	1.0 M KOH	155	115	[16]
NiCoFeP/C	1.0 M KOH	156	108	[17]
Ni@CoO@Co-MOFC	1 M KOH	138	59	This work

Table S4. Summary of Co and CoO-based materials for OER in alkaline media. (η_{10}-overpotential at 10 mA cm^{-2})

Catalysts	Electrolyte	η_{10}(mV)	Tafel slope (mV dec^{-1})	Refs.
N-CG–CoO	1 M KOH	340	71	[18]

NiCoP/rGO	1 M KOH	270	65.7	[19]
$Co_{0.5}Fe_{0.5}S$@N-MC	1 M KOH	410	159	[20]
Co@CoO_x NP	1 M KOH	289	68.9	[21]
Co@Co_3O_4/NC-2	0.1 M KOH	410	54.3	[22]
CS-Co/C-1000	1 M KOH	290	70	[23]
Co@NC-G-700	1 M KOH	322	73.7	[24]
Co/CoO@NC@CC	1 M KOH	284	76	[25]
CoN-400/CC	1 M KOH	251	75.4	[26]
CoP@PNC	1 M KOH	330	64	[27]
Co_3O_4/N-rmGO	1 M KOH	310	67	[28]
CoS_2(400)/N,S-GO	0.1 M KOH	380	75	[29]
CoP/rGO	1 M KOH	340	66	[30]
MnCoP NP	1 M NaOH	330	61	[31]
Ti foil/Nix$Co_{3-x}O_4$ NWs	1 M NaOH	~370	64	[32]
NiCoP/NF	1 M KOH	280	87	[33]
Co_3O_4@C/CP	1 M KOH	370	70	[34]
Ni@CoO@Co-MOFC	1 M KOH	247	51	This work

References

[1] Y. Hou, M. R. Lohe, J. Zhang, S. Liu, X. Zhuang and X. Feng, *Energy Environ. Sci.*, 2016, **9**, 478-483.

[2] H. Su, H.-H. Wang, B. Zhang, K.-X. Wang, X.-H. Li and J.-S. Chen, *Nano Energy*, 2016, **22**, 79-86.

[3] H. Fei, Y. Yang, Z. Peng, G. Ruan, Q. Zhong, L. Li, E. L. Samuel and J. M. Tour, *ACS Appl. Mater. Interfaces*, 2015, **7**, 8083-8087.

[4] F. Yang, P. Zhao, X. Hua, W. Luo, G. Cheng, W. Xing and S. Chen, *J. Mater. Chem. A*, 2016, **4**, 16057-16063.

[5] X. X. Liu, J. B. Zang, L. Chen, L. B. Chen, X. Chen, P. Wu, S. Y. Zhou and Y. H. Wang, *J. Mater. Chem. A*, 2017, **5**, 5865-5872.

[6] X. Zou, X. Huang, A. Goswami, R. Silva, B. R. Sathe, E. Mikmekova and T. Asefa, *Angew. Chem., Int. Ed. Engl.*, 2014, **53**, 4372-4376.

[7] M. Zeng, Y. Liu, F. Zhao, K. Nie, N. Han, X. Wang, W. Huang, X. Song, J. Zhong and Y. Li, *Adv. Funct. Mater.*, 2016, **26**, 4397-4404.

[8] Z.-H. Xue, H. Su, Q.-Y. Yu, B. Zhang, H.-H. Wang, X.-H. Li and J.-S. Chen, *Adv. Energy Mater.*, 2017, **7**, 1602355-1602362.

[9] H. Jin, J. Wang, D. Su, Z. Wei, Z. Pang and Y. Wang, *J. Am. Chem. Soc.*, 2015, **137**, 2688-2694.

[10] Z. Pei, Z. Tang, Z. Liu, Y. Huang, Y. Wang, H. Li, Q. Xue, M. Zhu, D. Tang and C. Zhi, *J. Mater. Chem. A*, 2018, **6**, 489-497.

[11] L. L. Feng, G. D. Li, Y. Liu, Y. Wu, H. Chen, Y. Wang, Y. C. Zou, D. Wang and X. Zou, *ACS Appl. Mater. Interfaces*, 2015, **7**, 980-988.

[12] C. Tang, R. Zhang, W. Lu, L. He, X. Jiang, A. M. Asiri and X. Sun, *Adv. Mater.*, 2017, **29**, 1602441-1602447.

[13] Y. Xie, M. Chen, M. Cai, J. Teng, H. Huang, Y. Fan, M. Barboiu, D. Wang and C. Y. Su, *Inorg. Chem.*, 2019, **58**, 14652-14659.

[14] J. Tian, Q. Liu, A. M. Asiri and X. Sun, *J. Am. Chem. Soc.*, 2014, **136**, 7587-7590.

[15] J. Wang, H. X. Zhong, Z. L. Wang, F. L. Meng and X. B. Zhang, *ACS Nano,* 2016, **10**, 2342-2348.

[16] M. Guo, S. Song, S. Zhang, Y. Yan, K. Zhan, J. Yang and B. Zhao, *ACS Sustainable Chemistry & Engineering*, 2020, **8**, 7436-7444.

[17] X. Wei, Y. Zhang, H. He, L. Peng, S. Xiao, S. Yao and P. Xiao, *Chem Commun*, 2019, **55**, 10896-10899.

[18] S. Mao, Z. Wen, T. Huang, Y. Hou and J. Chen, *Energy Environ. Sci.*, 2014, **7**, 609-616.

[19] J. Li, M. Yan, X. Zhou, Z.-Q. Huang, Z. Xia, C.-R. Chang, Y. Ma and Y. Qu, *Adv. Funct. Mater.*, 2016, **26**, 6785-6796.

[20] M. Shen, C. Ruan, Y. Chen, C. Jiang, K. Ai and L. Lu, *ACS Appl. Mater. Interfaces*, 2015, **7**, 1207-1218.

[21] J. Qi, W. Zhang and R. Cao, *Chem Commun*, 2017, **53**, 9277-9280.

[22] A. Aijaz, J. Masa, C. Rosler, W. Xia, P. Weide, A. J. Botz, R. A. Fischer, W. Schuhmann and M. Muhler, *Angew. Chem., Int. Ed. Engl.,* 2016, **55**, 4087-4091.

[23] J. Zhao, X. Quan, S. Chen, Y. Liu and H. Yu, *ACS Appl. Mater. Interfaces*, 2017, **9**, 28685-28694.

[24] X. Wen, X. Yang, M. Li, L. Bai and J. Guan, *Electrochim. Acta*, 2019, **296**, 830-841.

[25] K. Dai, N. Zhang, L. Zhang, L. Yin, Y. Zhao and B. Zhang, *Chem. Eng. J.*, 2021, **414**, 128804-128812.

[26] Z. Xue, J. Kang, D. Guo, C. Zhu, C. Li, X. Zhang and Y. Chen, *Electrochim. Acta*, 2018, **273**, 229-238.

[27] Z. Zhou, N. Mahmood, Y. Zhang, L. Pan, L. Wang, X. Zhang and J.-J. Zou, *J. Energy Chem.*, 2017, **26**, 1223-1230.

[28] Y. Liang, Y. Li, H. Wang, J. Zhou, J. Wang, T. Regier and H. Dai, *Nat. Mater.*, 2011, **10**, 780-786.

[29] P. Ganesan, M. Prabu, J. Sanetuntikul and S. Shanmugam, *ACS Catal.*, 2015, **5**, 3625-3637.

[30] L. Jiao, Y. X. Zhou and H. L. Jiang, *Chem Sci.*, 2016, **7**, 1690-1695.

[31] D. Li, H. Baydoun, C. N. Verani and S. L. Brock, *J. Am. Chem. Soc.*, 2016, **138**, 4006-4009.

[32] Y. Li, P. Hasin and Y. Wu, *Adv Mater*, 2010, **22**, 1926-1929.

[33] H. Liang, A. N. Gandi, D. H. Anjum, X. Wang, U. Schwingenschlogl and H. N. Alshareef, *Nano Lett.*, 2016, **16**, 7718-7725.

[34] X. Yang, H. Li, A.-Y. Lu, S. Min, Z. Idriss, M. N. Hedhili, K.-W. Huang, H. Idriss and L.-J. Li, *Nano Energy*, 2016, **25**, 42-50.